

Ultrafast demagnetization of ferromagnetic transition metals: The role of the Coulomb interaction

Michael Krauß, Tobias Roth, Sabine Alebrand, Daniel Steil, Mirko Cinchetti,
Martin Aeschlimann, and Hans Christian Schneider

Department of Physics and Research Center OPTIMAS, University of Kaiserslautern, Erwin-Schrödinger-Str. 46, 67653 Kaiserslautern, Germany

(Received 26 August 2009; revised manuscript received 18 October 2009; published 9 November 2009)

The Elliott-Yafet (EY) mechanism is arguably the most promising candidate to explain the light-induced ultrafast demagnetization dynamics in ferromagnetic transition metals on time scales on the order of 100 fs. So far, only electron-phonon (or impurity) scattering has been analyzed as the scattering process needed to account for the demagnetization. We show that an EY-like mechanism based on *electron-electron* scattering has the potential to explain time-resolved magneto-optical Kerr effect measurements on thin magnetic Co and Ni films, without reference to a “phononic spin bath.”

DOI: [10.1103/PhysRevB.80.180407](https://doi.org/10.1103/PhysRevB.80.180407)

PACS number(s): 75.10.Lp, 71.70.Ej, 78.47.J–

Current research in femtosecond magnetism is concerned with elucidating the fundamental mechanisms of light-induced spin dynamics as well as searching for potential applications in data processing.^{1–3} Despite important experimental studies employing various time-resolved techniques, no consensus on a microscopic understanding of ultrafast magnetization dynamics in ferromagnets has emerged. Rather, demagnetization dynamics is typically described in the framework of the phenomenological three-temperature model. In this model, temperatures are assigned to the electron, lattice, and spin “subsystems,” and the exchange of energy (and spin) is driven by the temperature differences between the respective subsystems. Although the three-temperature model provides an intuitive picture of demagnetization, its relation to the microscopic dynamics behind the demagnetization is still an active field of research.

The most popular candidate⁴ for the microscopic process behind light-induced ultrafast demagnetization is a mechanism of the Elliott-Yafet (EY) type.⁵ In the EY mechanism, the demagnetization arises because, in the presence of the spin-orbit (SO) interaction, spin is not a good quantum number, so that *any* momentum-dependent scattering mechanism changes the spin admixture when an electron is scattered from state $|\vec{k}\rangle$ to $|\vec{k}+\vec{q}\rangle$. So far, the scattering processes responsible for the EY mechanism have been assumed to be (quasi)elastic electron-phonon and electron-defect scattering in several theoretical and experimental studies.^{4,6–9} Unlike these papers, we analyze the ultrafast demagnetization in ferromagnetic metals due to an EY-like mechanism based exclusively on *electron-electron Coulomb scattering*. This scattering mechanism is not (quasi)elastic, so that the available phase space for transitions from minority to majority bands is much larger than for electron-phonon scattering, which can only cause transitions near points in the Brillouin zone where the bands are energetically close. As a proof of principle for the importance of electron-electron scattering for the demagnetization, we demonstrate quantitative agreement for the demagnetization time and magnetization quenching between time-resolved magneto-optical Kerr effect (TR-MOKE) measurements on Co and Ni, and numerical results based on the EY mechanism due to electron-electron scattering.

To resolve the electronic demagnetization dynamics on ultrafast time scales, we calculate the nonequilibrium momentum-resolved multiband electron dynamics at the level of Boltzmann scattering integrals, and we include the carrier excitation process. We therefore do not include true electronic correlation effects beyond carrier scattering nor coherent effects due to the optical excitation process.^{10–12}

For the description of our general approach, let us assume that the electronic single-particle energies ϵ_k^μ and wave functions $|\mu, \vec{k}\rangle$ —where the electronic band index μ runs over majority- and minority-spin bands, and the vector momentum is labeled by \vec{k} —are known from a band-structure calculation. Then the Coulomb and dipole matrix elements can be calculated and used as input for dynamical equations for the band- and momentum-resolved distribution functions n_k^μ . From these, the total magnetization of the system is obtained by $M = \sum_{\mu, \vec{k}} s_\mu n_k^\mu$, where $s_\mu = +1/2$ for majority and $s_\mu = -1/2$ for minority bands.¹³ The equation of motion determining the carrier distribution functions has the form¹⁴

$$\frac{\partial n_k^\mu}{\partial t} = \left. \frac{\partial n_k^\mu}{\partial t} \right|_{\text{opt}} + \left. \frac{\partial n_k^\mu}{\partial t} \right|_{\text{e-e}} + \left. \frac{\partial n_k^\mu}{\partial t} \right|_{\text{therm}}. \quad (1)$$

For the electron-electron Coulomb scattering we use the Boltzmann equation in the form

$$\begin{aligned} \left. \frac{\partial n_k^\mu}{\partial t} \right|_{\text{e-e}} &= \frac{2\pi}{\hbar} \sum_{\vec{\ell}, \vec{q}} \sum_{\mu_1 \mu_2 \mu_3} |V_{\mu_2 \mu_3}^{\mu \mu_1}(\vec{k}, \vec{\ell}, \vec{q}, \omega)|^2 \\ &\times [(1 - n_k^\mu) n_{k+\vec{q}}^{\mu_1} (1 - n_{\vec{\ell}+\vec{q}}^{\mu_2}) n_{\vec{\ell}}^{\mu_3} - \{(1 - n) \leftrightarrow n\}] \\ &\times \delta(\epsilon_k^\mu - \epsilon_{k+\vec{q}}^{\mu_1} + \epsilon_{\vec{\ell}+\vec{q}}^{\mu_2} - \epsilon_{\vec{\ell}}^{\mu_3}), \end{aligned} \quad (2)$$

where V is the dynamically screened Coulomb potential that depends on the initial and final states of the two scattering electrons $|\mu, \vec{k}\rangle \rightarrow |\mu_1, \vec{k}+\vec{q}\rangle$ and $|\mu_2, \vec{\ell}+\vec{q}\rangle \rightarrow |\mu_3, \vec{\ell}\rangle$, and $\hbar\omega = \epsilon_k^\mu - \epsilon_{k+\vec{q}}^{\mu_1}$. The optical excitation contribution in Eq. (1) is calculated by adiabatic elimination of the optical polarization,¹⁵

$$\left. \frac{\partial n_k^\mu}{\partial t} \right|_{\text{opt}} = \sum_{\nu \neq \mu} |\vec{d}_{\mu\nu}(\vec{k}) \cdot \vec{E}|^2 (n_k^\nu - n_k^\mu) g(\epsilon_k^\nu - \epsilon_k^\mu), \quad (3)$$

where \vec{E} is the classical electromagnetic field and the function $g(\hbar\omega)$ (peaked around the central frequency of the excitation pulse) models the spread of photon energies which can induce electronic transitions via the dipole matrix element $\vec{d}_{\mu\nu}(\vec{k})$ between states $|\nu, k\rangle$ and $|\mu, k\rangle$. Note that the EY mechanism based on electron-electron scattering is contained in Eqs. (1)–(3) if the Coulomb matrix elements include the spin-orbit interaction in the presence of the static lattice, so that scattering transitions change the average spin of the scattered electrons. The lattice effectively acts as a sink for the electronic angular momentum, which is “lost” from the electronic system by the spin nonconserving scattering processes described by Eq. (2). The important Coulomb and dipole matrix elements can, in principle, be determined from *ab initio* treatments,⁷ and parameter-free results can be achieved by a dynamical solution of Eqs. (1)–(3). However, due to the numerical complexity of the k -resolved Boltzmann scattering integral (2), we use a simplified model that contains parameters. We approximate the energy bands as spherically symmetric, $\epsilon_k^\mu = \epsilon_{|k|}^\mu$, and the screened Coulomb interaction as

$$V_{\mu_2\mu_3}^{\mu_1}(\vec{k}, \vec{\ell}, \vec{q}, \omega) = f_{\mu_1}^{\mu_1}(\vec{k}, \vec{q}) f_{\mu_3}^{\mu_2}(\vec{\ell}, \vec{q})^* v(q) \epsilon^{-1}(q, \omega), \quad (4)$$

where $f_{\mu}^{\mu'}(\vec{k}, \vec{q}) = \langle \mu, \vec{k} | \mu', \vec{k} + \vec{q} \rangle$ in general has a k dependence, but is taken here to be equal to 1 if $\mu = \mu'$ and α if $\mu \neq \mu'$. The parameter α is roughly comparable to the α parameter introduced by Yafet¹⁶ and calculated recently for metallic ferromagnets.⁷ In Eq. (4), $v(q)$ is the bare Coulomb potential and $\epsilon^{-1}(q, \omega)$ is the dynamical inverse dielectric function. Equation (4) can be shown to be valid if there are no short-range contributions to the Coulomb interaction,¹⁷ and we use this as an approximate explicit expression for the Coulomb matrix element of metals. Important dynamical screening effects are included via the Lindhard dielectric function $\epsilon(\vec{q}, \omega)$. In semiconductors, it has recently been demonstrated that an approach closely related¹⁴ to the one presented here leads to a parameter-free agreement for the spin dynamics in theory and experiment¹⁸ because quite accurate wave functions can be obtained using $\vec{k} \cdot \vec{p}$ theory. Finally, we assume that the optical excitation connects only majority and minority bands with each other, respectively, and we approximate the strength of the optical dipole matrix elements by a momentum- and band-independent constant \vec{d} . Although this is a drastic oversimplification, especially in view of the hybridization between s and p bands, it is in the same spirit as the approximations introduced for the band structure and the Coulomb interaction: the dependence on the electron vector momentum should either be included in all these quantities or modeled in a way that introduces the least amount of parameters in the model. In the minimal model of the present Rapid Communication, the electronic excitation after the optical pulse is therefore determined by the band structure, the central photon energy, and the width of pump pulse, as well as the fluence. These quantities are used as input for the numerical calculations.

The equilibration of the electronic system with the lattice is included in Eq. (1) via a relaxation time approximation $\partial n_k^\mu / \partial t|_{\text{therm}} = -(n_k^\mu - F_k^\mu) / \tau_{\text{phon}}$. Here, F_k^μ denotes the Fermi-Dirac distribution of electrons in band μ at lattice temperature. Note that in our model the demagnetization solely occurs due to Coulomb scattering, and that the electron-phonon interaction only leads to thermal equilibration, which actually restores the ground-state magnetization. The equilibration times $\tau_{\text{phon, Ni}} = 25$ ps and $\tau_{\text{phon, Co}} = 5$ ps are extracted from experiment by fitting the remagnetization dynamics. This assumption is based on the experimental observation that the time scale for energy equilibration due to electron-phonon interaction, which includes the effect of heat diffusion in a pragmatic way, is typically longer than the demagnetization time.

From the widespread point of view that one needs to transfer angular momentum away from the electronic “system” to explain electronic demagnetization, there is quite an important difference between our model based on electron-electron scattering and electron-phonon or impurity scattering. The latter couples directly to a bath and may transfer angular momentum to the lattice. We stress that the approximations introduced above do not implicitly introduce such a bath. To analyze angular-momentum conservation in detail in our model, the lattice dynamics due to the SO coupling needs to be included.

On the experimental side, a variety of techniques are available to excite and detect electron-spin dynamics.¹⁹ Here, we apply an all-optical strategy to trace the spin dynamics on femtosecond time scales. By means of the TR-MOKE in the longitudinal configuration we excite the ferromagnet by an ultrafast optical pump pulse and monitor the material response by a delayed and modified optical replica (probe pulse). The femtosecond pulses are generated by a Ti:sapphire multipass amplifier with 1 kHz repetition rate. We use s -polarized 50 fs 800 nm pump pulses at normal incidence, and s -polarized 50 fs 400 nm probe pulses under 45°. The samples are thin polycrystalline ferromagnetic layers: a 15 nm cobalt film deposited on MgO by dc sputtering and a 15 nm Ni film deposited on Si by electron-beam evaporation. The Ni film is capped by a 3 nm Ti layer; another 3 nm Ti layer acts as an adhesion promoter between the Ni film and the substrate.

Qualitatively, the ultrafast demagnetization occurs in our model in the following way. The electronic distributions in the unexcited ferromagnet are assumed to be Fermi-Dirac distributions determined by the lattice temperature and the band structure. The majority and the minority energy dispersions are spin split, so that a nonzero magnetization exists in equilibrium. The ultrafast optical excitation process creates nonequilibrium electronic distributions in bands accessible by the pump photon energy, and the electrons undergo intraband and interband Coulomb scattering processes. Due to our assumptions about the dipole matrix elements, the optical excitation process does not change the magnetization. The driving force for the demagnetization are interband scattering processes between the optically excited electrons, which lead to the redistribution of electrons from majority to minority bands as long as the optically excited electrons are spin po-

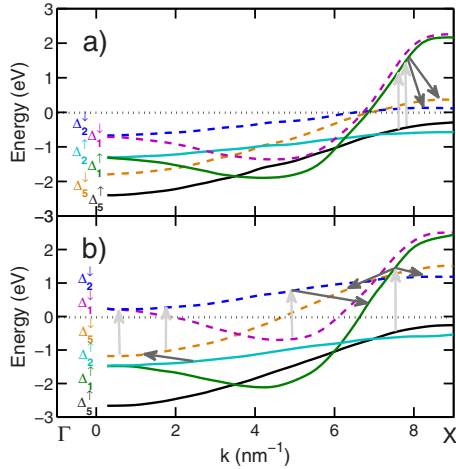


FIG. 1. (Color online) Band structure ϵ_k^μ of (a) Ni and (b) Co for majority (solid lines) and minority (dashed lines) electrons in Γ - X direction (Ref. 20). The Fermi energy E_F is set to zero. The arrows indicate a typical ultrafast demagnetization scenario: electrons are excited by an ultrashort laser pulse (vertical light gray arrows), which does not change the total magnetization. They relax via intraband and interband scattering (gray arrows). The latter scattering process leads to depolarization of the electrons.

larized. Remagnetization occurs due to equilibration at lattice temperature, because the ground-state magnetization is restored when the electrons settle down in the band minima.

For the numerical calculations we use as input for ϵ_k^μ a Korringa-Kohn-Rostoker density-functional theory result²⁰ for the Γ - X direction, which is then used for the whole Brillouin zone as if the band structure was spherically symmetric. These dispersions are plotted in Fig. 1. For an experimental and theoretical study of Co and Ni band structures that also discusses the nomenclature of the bands, see Ref. 21. The exciting laser pulse has a typical full width at half maximum of 50 fs, photon energy of 1.55 eV, and the fluence is numerically adjusted to be in qualitative agreement with an estimate of the absorption and the observed magnetization quenching. The pump pulse excites electrons into initially empty states above the Fermi energy E_F , as modeled by Eq. (3). Some numerical results obtained from Eq. (1) for the time- and momentum-resolved electron occupation for Ni are shown in Fig. 2. Since the distribution functions contain all the information on the dynamics on the single-particle level, we use them, together with the band structure shown in Fig. 1, to discuss the demagnetization scenario for Ni. Optical excitation by the ultrashort 1.55 eV excitation pulse is only possible for transitions from the Δ_2^\downarrow and Δ_3^\downarrow bands to the Δ_1^\uparrow (light gray arrows in Fig. 1). Figure 2(a) shows the nonequilibrium distributions created by the pump pulse. During and after the optical excitation of electrons in Δ_1^\uparrow , electron-electron scattering processes redistribute the carriers in and between the bands. In Figs. 2(c) and 2(d), the increasing number of electrons in Δ_2^\downarrow and Δ_3^\downarrow for positive time delays above $k=7 \text{ nm}^{-1}$ illustrates the dominant scattering pathways. Note that the scattering of electrons from majority to minority bands reduces the overall magnetization as the electronic contribution to the expectation value of the spin is

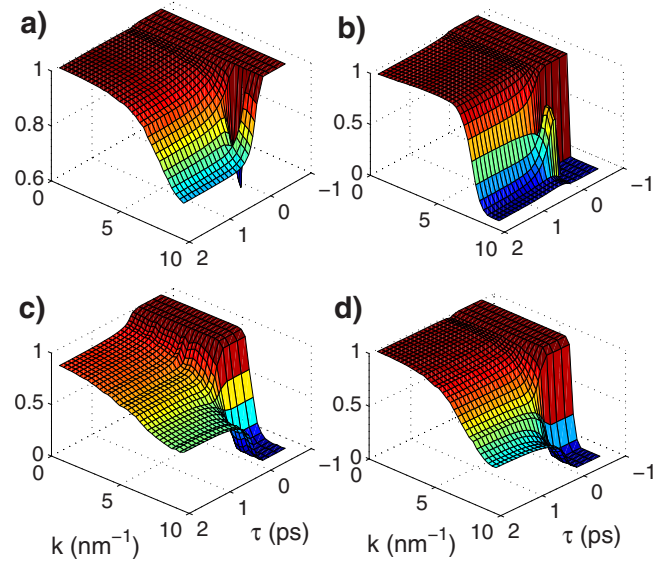


FIG. 2. (Color online) Dynamical distribution functions n_k^μ for four Ni bands (cf. Fig. 1). Electrons are excited from (a) bands Δ_2^\downarrow and Δ_3^\downarrow into (b) band Δ_1^\uparrow . Ultrafast demagnetization occurs by scattering into bands (c) Δ_2^\downarrow and (d) Δ_3^\downarrow .

altered. The processes responsible for the ultrafast loss of magnetic order in Ni start at more than 1 eV above the Fermi energy E_F and mainly take place near the X point. Remarkably, the demagnetization is almost completely dominated by the two transitions mentioned above, with the nonequilibrium scattering dynamics taking place over more than 100 fs [cf. Figs. 2(c) and 2(d)]. Electrons that are not scattered out of band Δ_1^\uparrow at high energies above the Fermi level accumulate in states close to the Fermi level because energy and momentum conservation requirements make outscattering processes inefficient. For completeness, we mention that band Δ_1^\downarrow does not play an important role in the demagnetization dynamics of Ni. An analysis of the electronic occupation in the different bands for Co along the same lines leads to the scenario as depicted in Fig. 1(b).

In Fig. 3, we plot the signal obtained from TR-MOKE measurements performed with the same pump fluence of 4 mJ/cm^2 and the calculated signal for Ni and Co. The magnetization quenching for Ni is significantly stronger than for Co. In our model this is explained by the band structure in combination with the optical excitation process, which yields a more efficient carrier excitation with 800 nm photons: in Ni mainly majority electrons are optically excited (see Fig. 1), so that all interband scattering processes above E_F lead to demagnetization. To obtain quantitative agreement between theory and experiment, we assume the same laser fluence for both materials and use the Elliott-Yafet factor α , introduced in Eq. (4), as a single fit parameter. We obtain $\alpha_{\text{Co}}=0.15$ and $\alpha_{\text{Ni}}=0.30$ together with the demagnetization times of $T_{\text{Co}}=215 \text{ fs}$ and $T_{\text{Ni}}=200 \text{ fs}$. The general trend $\alpha_{\text{Co}} < \alpha_{\text{Ni}}$ and the order of magnitude compare well with recent *ab initio* results for the α parameter.⁷ The results in Ref. 7 provide only a qualitative check for our fit parameters, because the *ab initio* results depend on the band-structure region, over which the wave-function coefficients are averaged. Last, but

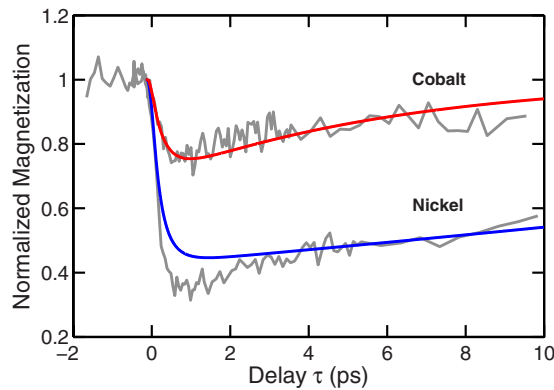


FIG. 3. (Color online) Normalized TR-MOKE rotation (gray curve) and calculated magnetization dynamics for Ni (blue curve) and Co (red curve). Assuming the same laser fluence, the choice of parameters $\alpha_{\text{Co}}=0.15$ and $\alpha_{\text{Ni}}=0.3$ yields good agreement between theory and experiment. The demagnetization times are $T_{\text{Co}}=215$ fs and $T_{\text{Ni}}=200$ fs. In the calculation, the stronger quenching of the magnetization for Ni is due to band-structure effects.

not least, we stress that the band-structure properties influ-

ence the microscopic dynamics sufficiently strongly to make it impossible to fit the Co measurements in Fig. 3 using the Ni band structure, and vice versa.

In conclusion, we presented evidence that ultrafast demagnetization in ferromagnets can occur due to an Elliott-Yafet mechanism based on electron-electron scattering in the presence of the spin-orbit interaction. Our model includes the optical excitation process and describes the scattering dynamics by Boltzmann scattering integrals for the momentum-dependent dynamical distribution functions in the various bands. At the single-particle level, this provides a general dynamical description of ultrafast demagnetization. Good agreement with our time-resolved magneto-optical Kerr measurements on Co and Ni is obtained by fitting the strength of the spin-orbit coupling parameter α and the fluence.

We acknowledge support from the DFG through the Graduiertenkolleg 792 “Nonlinear Optics and Ultrafast Processes” and the priority program SPP 1133, as well as from the NIC Jülich through a CPU time grant. We thank Christoph Döring for sample preparation, and M. Fähnle (MPI Stuttgart) for helpful discussions.

- ¹A. Vaterlaus, T. Beutler, and F. Meier, *Phys. Rev. Lett.* **67**, 3314 (1991).
- ²E. Beaupaire, J.-C. Merle, A. Daunois, and J.-Y. Bigot, *Phys. Rev. Lett.* **76**, 4250 (1996).
- ³H.-S. Rhie, H. A. Dürr, and W. Eberhardt, *Phys. Rev. Lett.* **90**, 247201 (2003).
- ⁴B. Koopmans, J. J. M. Ruigrok, F. Dalla Longa, and W. J. M. de Jonge, *Phys. Rev. Lett.* **95**, 267207 (2005).
- ⁵I. Žutić, J. Fabian, and S. Das Sarma, *Rev. Mod. Phys.* **76**, 323 (2004).
- ⁶B. Koopmans, H. H. J. E. Kicken, M. van Kampen, and W. J. M. de Jonge, *J. Magn. Magn. Mater.* **286**, 271 (2005).
- ⁷D. Steiauf and M. Fähnle, *Phys. Rev. B* **79**, 140401(R) (2009).
- ⁸M. Cinchetti, M. Sanchez Albaneda, D. Hoffmann, T. Roth, J. P. Wüstenberg, M. Krauß, O. Andreyev, H. C. Schneider, M. Bauer, and M. Aeschlimann, *Phys. Rev. Lett.* **97**, 177201 (2006).
- ⁹C. Stamm *et al.*, *Nature Mater.* **6**, 740 (2007).
- ¹⁰G. P. Zhang and W. Hübner, *Phys. Rev. Lett.* **85**, 3025 (2000).
- ¹¹G. Lefkidis and W. Hübner, *Phys. Rev. B* **76**, 014418 (2007).
- ¹²J.-Y. Bigot, M. Vomir, and E. Beaupaire, *Nat. Phys.* **5**, 515

(2009).

- ¹³In principle the contributions of the single particle states $|\mu, \vec{k}\rangle$ to the total spin is momentum dependent (Ref. 14), $s_{\mu} = s_{\mu, \vec{k}}$, and can be determined from band-structure calculations.
- ¹⁴M. Krauß, M. Aeschlimann, and H. C. Schneider, *Phys. Rev. Lett.* **100**, 256601 (2008).
- ¹⁵W. Schäfer and M. Wegener, *Semiconductor Optics and Transport Phenomena* (Springer, New York, 2002).
- ¹⁶Y. Yafet, in *Solid State Physics*, edited by F. Seitz and D. Turnbull (Academic, New York, 1963), Vol. 14, p. 1.
- ¹⁷G. E. Pikus and G. L. Bir, *Sov. Phys. JETP* **33**, 208 (1971).
- ¹⁸D. J. Hilton and C. L. Tang, *Phys. Rev. Lett.* **89**, 146601 (2002).
- ¹⁹M. Aeschlimann, M. Bauer, S. Pawlik, W. Weber, R. Burgermeister, D. Oberli, and H. C. Siegmann, *Phys. Rev. Lett.* **79**, 5158 (1997).
- ²⁰*Magnetic Transition Metals*, edited by A. Goldman, Landolt-Börnstein, New Series, Group III, Vol. 23, Pt. C2 (Springer, Berlin, 1999).
- ²¹M. Hochstrasser, N. Gilman, R. F. Willis, F. O. Schumann, J. G. Tobin, and E. Rotenberg, *Phys. Rev. B* **60**, 17030 (1999).